JOES: An application software for Judd-Ofelt analysis from Eu^{3+} emission spectra

Aleksandar Ćirić[a], Stevan Stojadinović[a,*], Milica Sekulić[b], Miroslav D. Dramićanin[b]

[a] University of Belgrade, Faculty of Physics, Studentski trg 12–16, Belgrade 11000, Serbia
[b] University of Belgrade, Vinča Institute of Nuclear Sciences, P.O. Box 522, Belgrade 11001, Serbia

https://doi.org/10.1016/j.jlumin.2018.09.048

Journal of Luminescence 205 (2019) 351–356

* Corresponding author. *E-mail address:* sstevan@ff.bg.ac.rs (S. Stojadinović).

A B S T R A C T

PREPRINT

In this paper we will be presenting JOES (Judd-Ofelt from Emission Spectra), an application software for cal-culation of the Judd-Ofelt intensity parameters and derived quantities from the emission spectra of Eu^{3+} doped materials. The program is written to be user friendly and it requires no previous experience in the field of study. This Free and Open-Source program written in JAVA, works on Windows, Linux and MAC OS operating systems. Program has been tested on three europium doped oxides with good luminescent properties: TiO_2:Eu^{3+}, ZrO_2:Eu^{3+} and Nb_2O_5:Eu^{3+}. We wish to give to the researchers this theoretical tool which can make the cal-culations easier, faster and more reliable.

1. Introduction

The rare earth elements (RE) have properties that are re-volutionizing modern science, technology and everyday life [1]. The main interest in RE lies in their photoluminescent (PL) properties, and the number of research papers on lanthanides shows an overall growing trend (see Fig. 1), with an exponential growth in the number of research papers investigating their application.

From the absorption or luminescence spectra, Judd-Ofelt theory (JO) has the ability to predict oscillator strengths, luminescence branching ratios, excited state radiative lifetimes, and estimates of quantum efficiencies, by using only three parameters. Thus, it has be-come a centerpiece in RE optical spectroscopy [2]. Unfortunately, the theory itself is complex, and the calculation by hand is a cumbersome process that can be easily overcome with an appropriate application software.

The usual way for calculating JO parameters of solids with doped trivalent RE ions is with the absorption spectra, and it involves a complicated algorithm, best described in Ref. [2], and supported by the RELIC application software [3].

Europium is unique among RE elements in a way that JO analysis can be done with the emission as well as with the absorption spectra. Apart from the simpler algorithm, PL methods are 3 orders of magnitude more sensitive than in absorption spectroscopy [4]. LUMPAC is a software package that can calculate JO parameters from the emission spectra, but it is limited to only two intensity parameters and it lacks the ability to calculate many JO derived quantities [5]. Recently, simple scripts using the MathCad 14® program have been presented from which one can easily obtain the Ω_2 and Ω_4 experimental intensity parameters by using the areas under the emission curves and energy barycenters of the $^5D_0 \rightarrow {}^7F_2$ and $^7F_4$ transitions using the magnetic dipole $^5D_0 \rightarrow {}^7F_1$ one as the reference. However, MathCad 14® program is a commercial software and operates only on MS Windows. To over-come these limitations, the JOES software was created. Containing the vast database of refractive indexes, it requires only a single file to cal-culate Judd-Ofelt intensity parameters, branching ratios, radiative transition probabilities, barycenter energies, nonradiative transition probability, lifetimes, cross-sections, quantum efficiency and sensitiza-tion efficiency.

In the next section the JO theory for the emission spectra of Eu^{3+} doped materials is briefly reviewed. Section 3 gives information on how the software uses the theory for calculations and is a short introduction into its user interface (UI). Section 4 presents the results obtained from the emission spectra of three different hosts, doped with different concentrations of europium. Finally, the last section presents the ad-ditional information that can be obtained from the emission spectra of europium doped compounds by JOES application software.

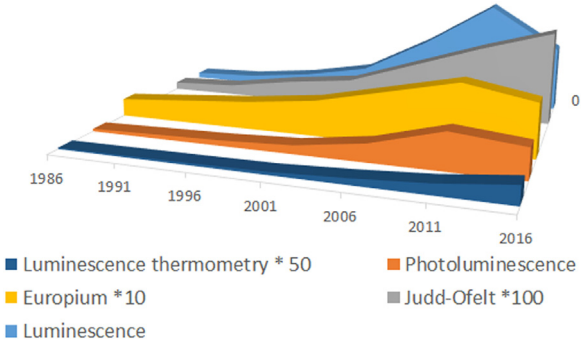

Fig. 1. A number of papers found for the search term using Google Scholar, published in the 5-year intervals [31].

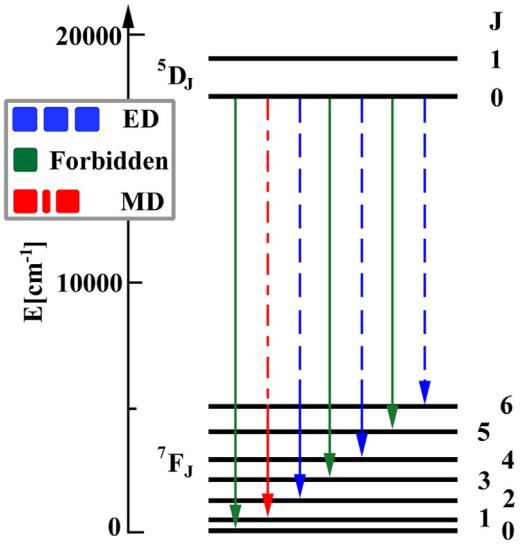

Fig. 2. Transitions from the first excited level to the ground level of europium.

2. The theory

2.1. JO parameters

The uniqueness of europium lies in its magnetic dipole (MD) transition, $^5D_0 \rightarrow {}^7F_1$, which dipole strength is independent on the environment. Thus, it can be calculated exactly and used as a reference for transitions originating from $^5D_0$ [6,7] (1 esu = $N^{-5/2}$ cm):

$$D_{MD} = 9.6{\cdot}10^{-42}\ \text{esu}^2\ \text{cm}^2 = 9.6{\cdot}10^{-6}\ \text{Debye}^2 \quad (1)$$

Another uniqueness is that all the reduced matrix elements, $|\langle J|U^\lambda|J'\rangle|^2$ abbreviated as U^λ, for electric dipole (ED) transitions originating from $^5D_0$ level are zero, except to the levels $^7F_\lambda$, where $\lambda = 2, 4, 6$ [8]: $U^2 = 0.0032$, $U^4 = 0.0023$, $U^6 = 0.0002$. One should note that there is a dispute in the scientific community regarding a value of the squared reduced matrix element of the unit tensor operator U^6 since Carnall et al. did not assign any value for this reduced matrix element in their tables. Here, we have calculated 0.0002 value for U^6 using the RELIC software [2,3] for average values of Slater's integrals and s-o parameters ($F_2 = 381\ \text{cm}^{-1}$, $F_4 = 56\ \text{cm}^{-1}$, $F_6 = 6\ \text{cm}^{-1}$, and $z = 1331\ \text{cm}^{-1}$). The same result has been obtained by Dejneka et al. [22] when analyzing Eu^{3+} emission in fluoride glasses. Then, the calculation of JO parameters from the ratio of the integrated intensities of transitions $^5D_0 \rightarrow {}^7F_\lambda$ and MD transition $^5D_0 \rightarrow {}^7F_1$ can be accomplished from [9]:

$$\Omega_\lambda = \frac{D_{MD}\tilde{\nu}_1^3}{e^2\tilde{\nu}_\lambda^3 U^\lambda}\frac{9n_1^3}{n_\lambda(n_\lambda^2+2)^2}\frac{J_\lambda}{J_1} \quad (2)$$

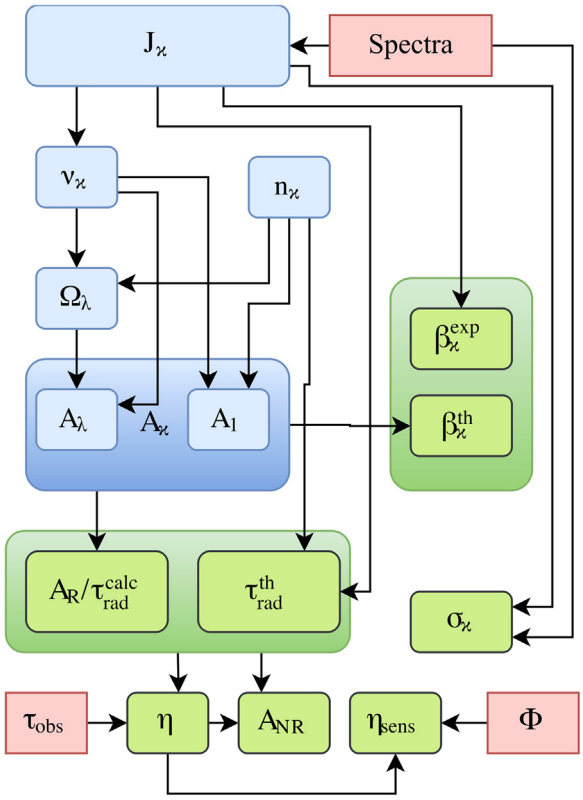

Fig. 3. The flow chart of the steps and requirements for the calculation of JO and derived quantities. Red – experimentally obtained quantities, Blue – steps, Green – derived quantities (For interpretation of the references to color in this figure legend, the reader is referred to the web version of this article.).

where $J_\kappa = \int I_\kappa(\tilde{\nu})d\tilde{\nu}$ is integrated intensity of the transition $^5D_0 \rightarrow {}^7F_\kappa$, and $\tilde{\nu}_\kappa$ is the average wavenumber in cm^{-1}, the barycenter of the transition to the $^7F_\kappa$ level: $\tilde{\nu}_\kappa = \int \tilde{\nu} I_\kappa(\tilde{\nu})d\tilde{\nu}/J_\kappa$, where $\kappa = 1, 2, 4, 6$.

As the refractive index, n, is wavelength dependent, its value should be taken from the Sellmeier's equation or measured at the exact wavelength or wavenumber that corresponds to the barycenter: $n_\kappa \equiv n(\tilde{\nu}_\kappa)$.

2.2. Radiative transition probabilities

Dipole strengths for ED transitions, for the unique case of Eu^{3+}, are given by $D_{ED}^\lambda = e^2\Omega_\lambda U^\lambda$, where $e = 4.803{\cdot}10^{-10}$ esu is the elementary charge. Now radiative transition probabilities, A_κ can be calculated from JO parameters [10,11]:

$$A_\lambda = \frac{64\pi^4\tilde{\nu}_\lambda^3}{3h}\frac{n_\lambda(n_\lambda^2+2)^2}{9}D_{ED}^\lambda,\ A_1 = \frac{64\pi^4\tilde{\nu}_1^3}{3h}n_1^3 D_{MD} \quad (3)$$

where $h = 6.63{\cdot}10^{-27}$ erg s is the Planck constant (1 erg = 10^{-5} N cm).

Note that in JO model $A(^5D_0 \rightarrow {}^7F_J, J = 0, 3, 5) = 0$, since those transitions are forbidden (see Fig. 2). Thus, the total radiative transition is given by: $A_R = \sum A_\kappa$.

2.3. Derived quantities

Derived quantities from JO theory provide the information about the practical applicability of the investigated material. Quantities calculated here are: radiative lifetime, branching ratios, stimulated emission cross section, luminescence quantum efficiency, optical gain, quantum yield and the sensitization efficiency.

The lifetime is the time after which the population of an excited state has decayed to 1/e, or 36.8%, of the initial population. Higher emission probabilities and more frequent transitions from a level lead to faster decay and shorter lifetimes. The calculated radiative lifetime is

(a)

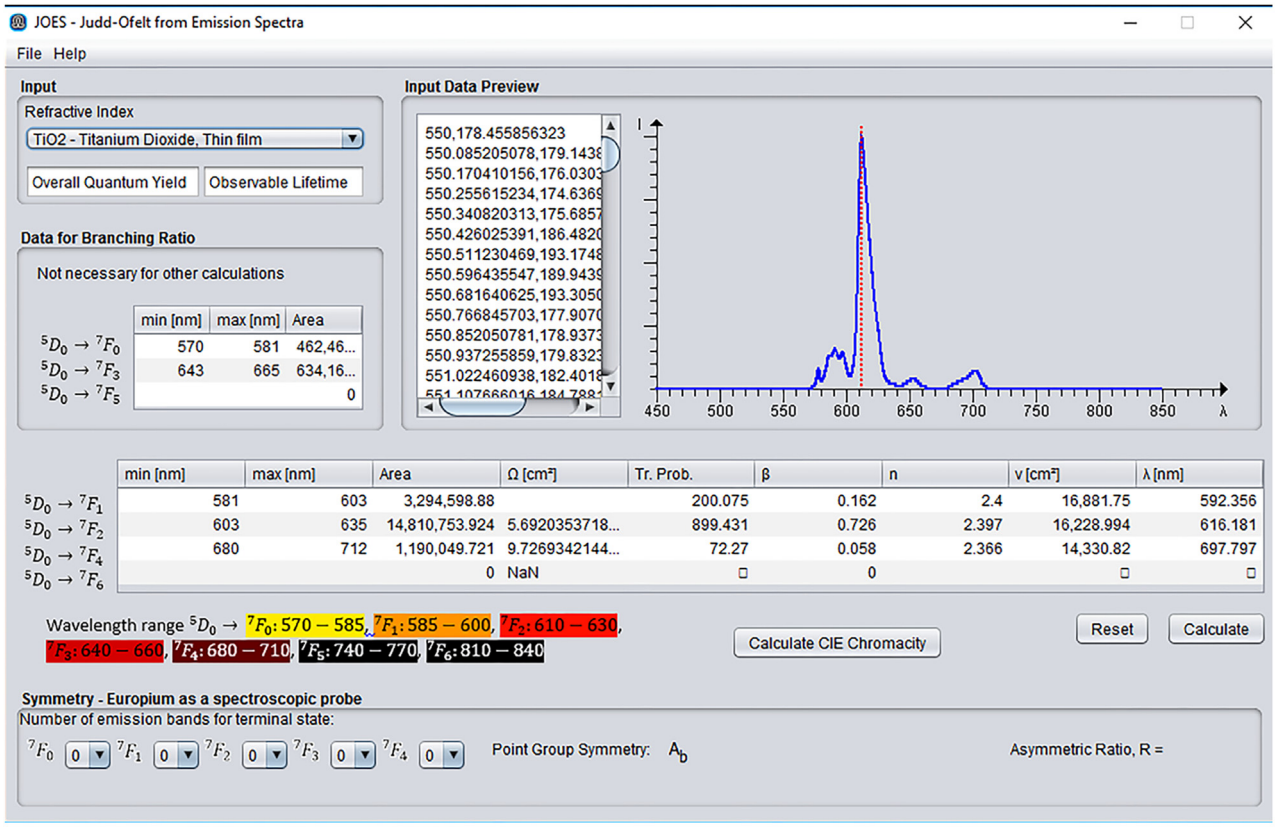

(b)

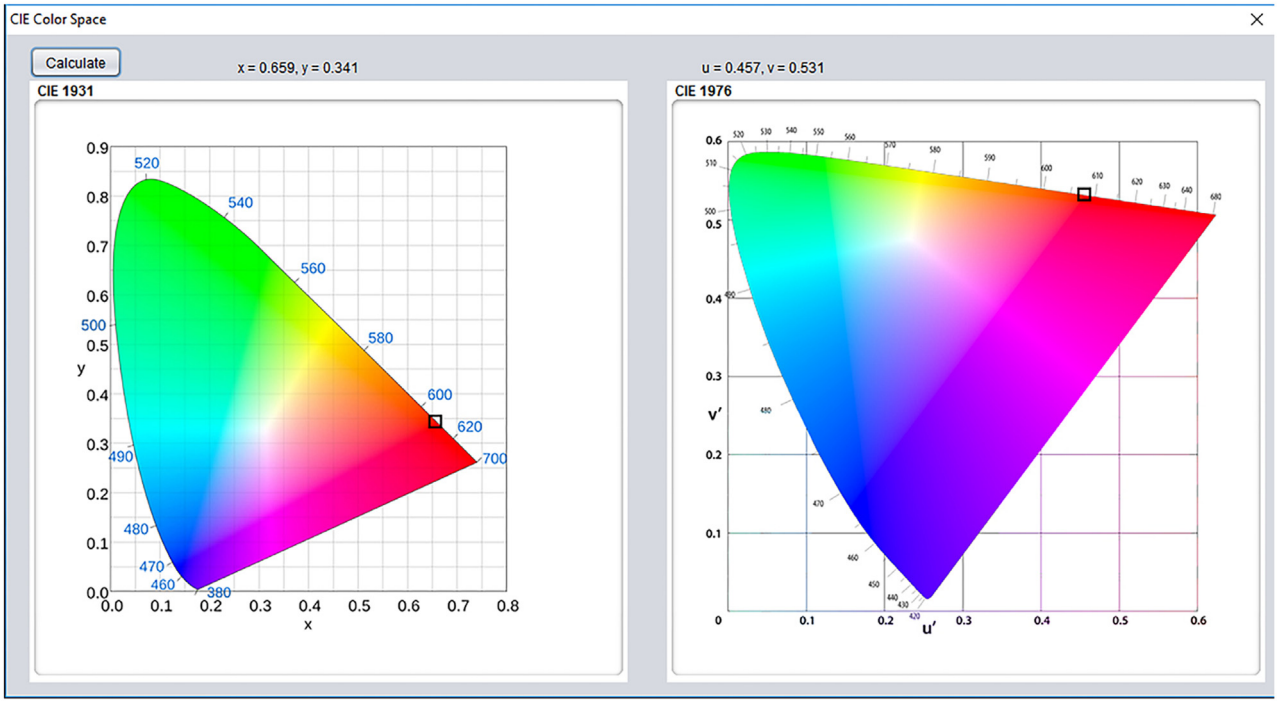

Fig. 4. (a) UI of JOES, (b) UI for calculation and graphical plot of CIE 1931 and CIE 1976 chromaticity coordinates.

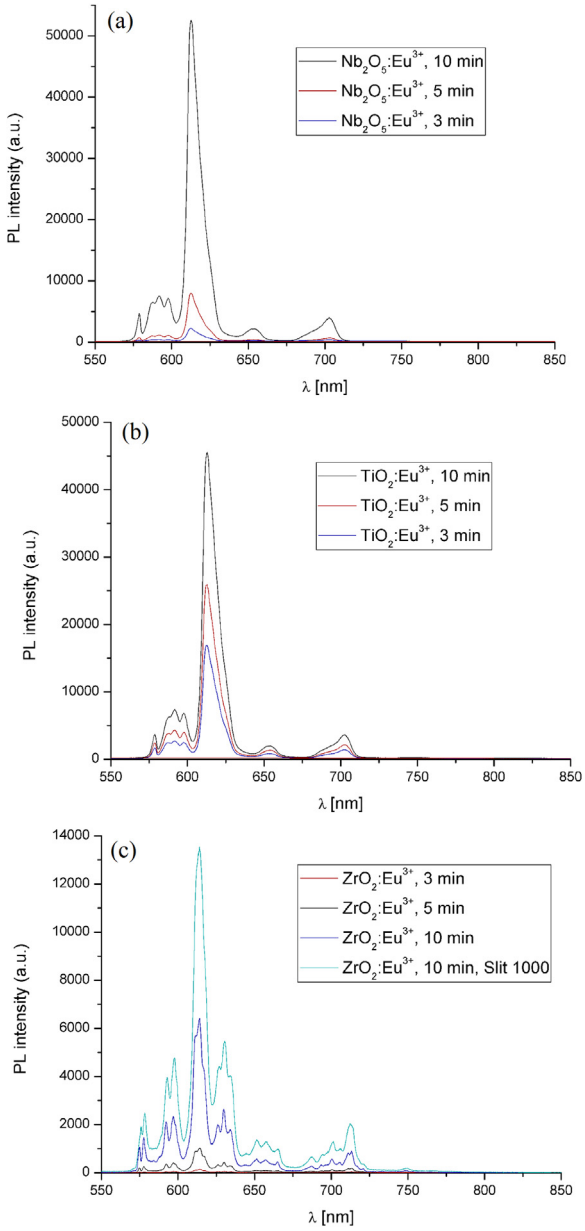

Fig. 5. Evolution of PL spectra of Eu^{3+} doped (a) Nb_2O_5, (b) TiO_2 and (c) ZrO_2 hosts, at various PEO times, excited at 464 nm.

equal to the inverse of the total radiative lifetime: $\beta_\kappa^{\text{th}} = A_\kappa / \sum A_\kappa$. Experimentally observed lifetime, τ_{obs}, takes into account both radiative and non-radiative rates, and is given by: $1/\tau_{\text{obs}} = A_R + A_{NR}$. It can be determined from the emission intensity decay following pulse excitation, i.e. by the time-domain method [12]. The width of the pulse should be shorter than the lifetime of the excited state. For lifetime measurements of Eu compounds typically a microsecond flash lamp is used, at wavelength obtained from the excitation spectra. In the case of single-exponential decay, intensity is equal to: $I(t) = I(0)\exp(-t/\tau_{\text{obs}})$.

The observable lifetime can now be calculated from the slope of a plot of *ln I(t)*. In case that the decay curve is not single-exponential, the lifetime can be numerically evaluated with the average lifetime [6]: $\tau_{\text{obs}} = \int_0^\infty tI(t)dt / \int_0^\infty I(t)dt$.

Theoretical radiative lifetime can obtained directly from the spectrum, and is given by [13]:

$$\tau_{\text{rad}}^{\text{th}} = \frac{n_1^{-3}}{14.65} \frac{J_1}{J_{\text{tot}}} \tag{4}$$

However, note that this is just a theoretical model for which the real values might slightly vary, and the two values for the radiative lifetime should be compared.

Branching ratios can be used to predict the relative intensities of all emission lines originating from a given excited state [14]. Theoretical branching ratio is obtained from the JO theory: $\beta_\kappa^{\text{th}} = A_\kappa / \sum A_\kappa$.

These branching ratios do not include transitions other than to $^7F_\kappa$, and this is justified by the analysis that indicates that these transitions "borrow" their intensity from the hypersensitive transition through higher order perturbations of the crystal field [15]. Branching ratios can also be obtained directly from the emission spectra as a ratio of integrated intensities: $\beta_\kappa^{\text{exp}} = J_\kappa / J_{\text{tot}}$.

The two types of branching ratios should be compared. Emission level with $\beta > 50\%$ is a potential laser emission transition [2]. The most important parameter determining the potential laser performance is the stimulated emission cross section, given by [7,14,16]:

$$\sigma_\kappa(\lambda_p) = \frac{\lambda_p^4}{8\pi c n_p^2} \frac{\max I_\kappa}{\int I_\kappa d\lambda} A_\kappa \tag{5}$$

where λ_p is the wavelength of the peak κ, and n_p is the refractive index at λ_p.

Luminescence quantum efficiency (or intrinsic quantum yield), η, is by definition the ratio of the number of photons emitted to the number of photons absorbed. For RE ions it is also equal to the ratio of the observed lifetime to the radiative lifetime [9]:

$$\eta = \frac{\tau_{\text{obs}}}{\tau_{\text{rad}}} \tag{6}$$

Overall quantum yield, Φ, can be determined if the quantum yield of the investigated sample is compared with that of a reference sample, e.g. $Y_2O_3{:}Eu^{3+}$. The knowledge of Φ can give us the sensitization efficiency: $\eta_{\text{sens}} = \Phi/\eta$.

To obtain the desired derived quantity it is necessary to follow the algorithm presented in Fig. 3.

Finally, one should note that JO analysis accounts only the forced electric dipole mechanism contributions when calculating non-radiative energy transfer rates (not considering the polarizability dependent dynamic coupling mechanisms). Therefore, one should be aware of the importance of theoretical calculations based on structural data, crystal field and dynamic coupling models, as is the case with the LUMPAC software [5].

3. Application software

3.1. Refractive index

For better accuracy the refractive indexes should be obtained at the wavenumber of the peak's barycenter instead of applying the constant value for all transitions [7]. Unless a user enters the values manually, the program takes refractive indexes in two forms: Sellmeier's equations or calculated numerically, from values obtained from the refractive index database [17].

3.2. Derived quantities

Equations for radiative transition probability in the simplest form are:

$$A_\lambda = 8.034 \cdot 10^9 \cdot \tilde{\nu}_\lambda^3 n_\lambda (n_\lambda^2+2)^2 \Omega_\lambda U^\lambda \tag{7}$$

$$A_1 = 3.009 \cdot 10^{-12} \cdot \tilde{\nu}_1^3 n_1^3 \tag{8}$$

The equation for cross sections in cm^2, which is the function of the wavelength, given in nm, is:

$$\sigma_\kappa(\lambda_p) = \frac{\lambda_p^4}{23.984\ \pi \cdot n_p^2} \frac{\max I_\kappa}{\int i_\kappa d\lambda \cdot 10^{-7}} A_\kappa \cdot 10^{-31} \tag{9}$$

Table 1
JOES output data for TiO_2:Eu^{3+}, ZrO_2:Eu^{3+} and Nb_2O_5:Eu^{3+} at various PEO times.

Host	ZrO_2			TiO_2			Nb_2O_5		
PEO time [min]	10	5	3	10	5	3	10	5	3
Concentration [%]	0.44	0.33	0.17	0.34	0.20	0.15	1.42	1.11	0.62
$\Omega_2 \cdot 10^{20}$ [cm^2]	4.836	4.645	4.567	5.692	5.453	5.295	6.124	5.810	4.677
$\Omega_4 \cdot 10^{20}$ [cm^2]	1.306	1.857	4.812	0.972	1.069	0.963	1.022	1.350	2.712
β_{exp} ($^5D_0 \rightarrow {}^7F_1$)	0.174	0.169	0.130	0.161	0.164	0.169	0.156	0.155	0.156
β_{exp} ($^5D_0 \rightarrow {}^7F_2$)	0.606	0.565	0.426	0.726	0.706	0.709	0.734	0.696	0.560
β_{exp} ($^5D_0 \rightarrow {}^7F_4$)	0.078	0.108	0.217	0.058	0.065	0.060	0.058	0.076	0.155
β_{th} ($^5D_0 \rightarrow {}^7F_1$)	0.202	0.200	0.168	0.170	0.175	0.180	0.164	0.167	0.179
β_{th} ($^5D_0 \rightarrow {}^7F_2$)	0.705	0.670	0.550	0.767	0.754	0.754	0.774	0.749	0.642
β_{th} ($^5D_0 \rightarrow {}^7F_4$)	0.091	0.128	0.280	0.061	0.069	0.064	0.061	0.082	0.177
A ($^5D_0 \rightarrow {}^7F_1$) [$s^{-1}$]	143.58	143.48	143.59	200.07	200.46	200.39	183.28	183.35	183.68
A ($^5D_0 \rightarrow {}^7F_2$) [$s^{-1}$]	499.21	479.06	469.58	899.43	861.83	837.27	863.23	819.23	658.36
A ($^5D_0 \rightarrow {}^7F_4$) [$s^{-1}$]	64.54	91.96	239.30	72.26	79.63	71.63	68.07	90.22	182.27
v ($^5D_0 \rightarrow {}^7F_1$) [$cm^{-1}$]	16,811	16,807	16,811	16,881	16,892	16,890	16,883	16,886	16,896
v ($^5D_0 \rightarrow {}^7F_2$) [$cm^{-1}$]	16,172	16,167	16,151	16,228	16,229	16,231	16,232	16,234	16,226
v ($^5D_0 \rightarrow {}^7F_4$) [$cm^{-1}$]	14,211	14,219	14,239	14,330	14,339	14,333	14,323	14,336	14,363
τ_{th} [ms]	1.186	1.151	0.885	0.797	0.812	0.838	0.841	0.841	0.844
τ_{calc} [ms]	1.413	1.399	1.173	0.853	0.875	0.901	0.971	0.915	0.976
τ_{obs} [ms]	0.883	0.869	0.812	0.578	0.587	0.588	0.506	0.506	0.551
σ ($^5D_0 \rightarrow {}^7F_1$)$\cdot 10^{22}$ [cm^2]	5.336	5.623	5.485	3.587	3.456	3.516	3.422	0.449	0.757
σ ($^5D_0 \rightarrow {}^7F_2$)$\cdot 10^{22}$ [cm^2]	15.118	14.693	13.554	23.731	22.565	22.504	25.241	3.182	4.487
σ ($^5D_0 \rightarrow {}^7F_4$)$\cdot 10^{22}$ [cm^2]	3.034	3.830	6.702	2.628	2.639	2.562	2.634	0.502	1.019
η	0.744	0.754	0.917	0.724	0.722	0.700	0.601	0.602	0.653
Asymmetric ratio	3.756	3.607	3.541	4.859	4.665	4.552	3.756	3.607	3.541

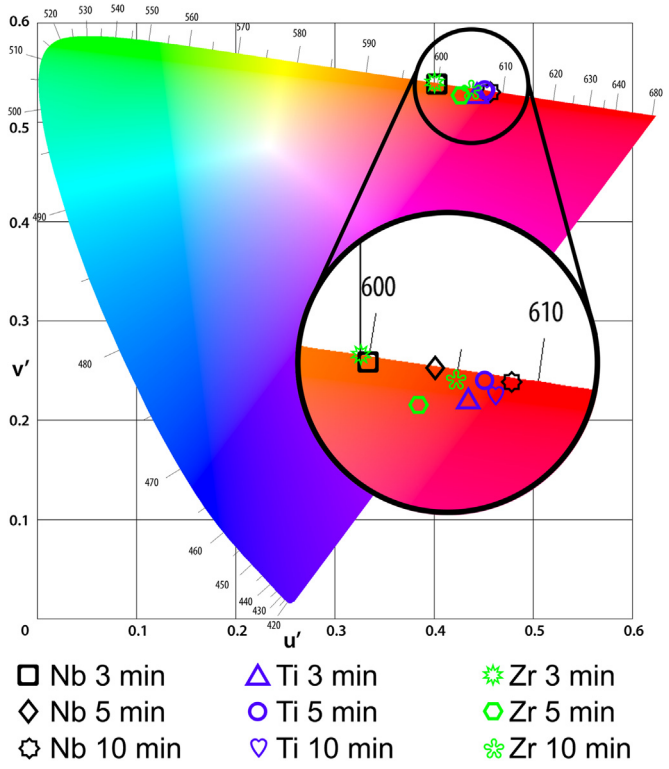

Fig. 6. CIE 1976 chromaticity diagram with PL plot of all three compounds given in various Eu^{3+} concentrations.

3.3. UI

The UI of JOES is presented in Fig. 4. After the input of the comma separated value (CSV) file, with points obtained from the spectrofluorometer (the CSV file can be exported from the Origin [18]), the graph and the table of intensities vs. wavelengths appear in the *Input Data Preview* panel. The user is asked to choose the material from the database with over 150 entries, or to manually input the refractive indexes in the table.

In the main table, peak bounds must be entered for all but the $^5D_0 \rightarrow {}^7F_6$ transition, since it lies outside the visible spectrum and is very weak in many materials. The inputs for the *Overall Quantum Yield* and the *Observable Lifetime* are optional entries and are required only for calculations of the derived quantities. A complete set of results the program outputs to a text file. Instructions are provided in more detail in the help file within the application software.

4. JO analysis of TiO_2, ZrO_2 and Nb_2O_5 doped with Eu^{3+}

Testing samples are prepared by the plasma electrolytic process (PEO), described in detail in Refs. [19–21], from the thin foils of pure Ti, Zr and Nb. The thin film of doped oxide forms on the foil surface. Various concentrations of doped europium are provided with the different PEO process time. The corrected spectra, presented in Fig. 5. is recorded by Fluorolog-3 Model FL3-221 spectrofluorimeter system (Horiba-Jobin Yvon), excited with OPO laser at 464 nm, and recorded by a CCD detector. The transition to the $^7F_6$ level is not observed in any of the spectra.

The data from JOES application software is presented in Table 1. The calculated data gives the information about the luminescent and structural properties of the material, which is the discussion beyond the scope of this paper. JO parameters and the derived quantities obtained from the absorption spectrum are generally accepted to be accurate within 20% [22,23], from the emission spectrum within 10% [6]. By comparing the calculated with theoretical values for the branching ratio and radiative lifetime, it is evident that they match within the desired 10% for all three samples, which is an indication of the accuracy of the JOES application software.

5. Additional features

Additionally, JOES application software can determine chromaticity from spectrum or exploit the Eu^{3+} ability to be used as a spectroscopic probe to determine the site symmetry.

5.1. Spectroscopic probe

By counting the number of crystal-field components that can be observed for the transitions $^5D_0 \rightarrow {}^7F_J$, the point group symmetry of the Eu^{3+} site can be determined, as described by K. Binnemans and C. Gorller-Walrand in Ref. [24]. The user needs to enter the number of observed peaks for the given terminal state and the program output will provide the possible point group symmetry.

The problem with the site symmetry identification often arises due to the overlapping of the peaks. Often the weaker overlapping peak appears as a shoulder to the more intense peak. The other complication arises because of the overlapping with the transitions from higher excited states. This problem can be resolved by time-gated spectroscopy or by measuring at lower temperatures. Multiple symmetries in the program output mean that the information on the polarization of the transitions is required to assign a particular symmetry group, which is beyond this project's scope.

The asymmetric ratio gives a measure of the degree of distortion from the inversion symmetry of the local environment of the Eu^{3+} ion in a matrix [25]. It is equal to the ratio of integrated intensities of the hypersensitive and magnetic dipole transitions [26]. As the Eu^{3+} concentration increases, more lattices become deviated and lose symmetry. In all three hosts investigated in this paper, the asymmetric ratios calculated by JOES increase with increasing Eu^{3+} concentrations, as predicted by the theory.

5.2. Chromaticity

After the spectrum data has been loaded into the JOES application software, the calculation of the Commission International De I-Eclairage (CIE 1931 and CIE 1976) coordinates are evaluated and plotted (Fig. 6.). The color matching curves are approximated as given in Ref. [27] and calculated as explained in Refs. [28,29].

From the spectra of the Eu^{3+} doped TiO_2, ZrO_2 and Nb_2O_5, it is evident the existence of the chromatic shift towards higher wavelengths proportional to the europium concentration. The similar results are reported in Ref. [30]. These results indicate that all three materials can be used as a red phosphor for LED or display applications.

6. Conclusion

JOES is the complete package for calculation of Judd-Ofelt parameters and derived quantities from the emission spectra of europium doped compounds. To our knowledge, it is the only application software that facilitates the complete study of this type, and is available free of charge (with the only obligation, if used, to reference to this paper) at the web site: https://sites.google.com/view/juddofelt/, as well as its source files. To our knowledge, until now, there has been no Judd-Ofelt analysis on the materials prepared by the PEO process. The results obtained for the three investigated samples stand as the guarantee of the accuracy of the calculated results.

This computational tool brings the power of the Judd-Ofelt theory without the necessary theoretical knowledge, and we offer it to the other experimental research teams interested in luminescent systems.

Acknowledgements

This work is supported by the Ministry of Education, Science and Technological Development of the Republic of Serbia under Project No. 171035 and 45020.

References

[1] L. Smentek, Judd-Ofelt theory - the golden (and the only one) theoretical tool of f-electron spectroscopy, Comput. Methods Lanthan. Actin. Chem. John Wiley & Sons Ltd, Chichester, UK, 2015, pp. 241–268, , https://doi.org/10.1002/9781118688304.ch10.
[2] M.P. Hehlen, M.G. Brik, K.W. Krämer, 50th anniversary of the Judd–Ofelt theory: an experimentalist's view of the formalism and its application, J. Lumin. 136 (2013) 221–239, https://doi.org/10.1016/j.jlumin.2012.10.035.
[3] M.P. Hehlen, Rare Earth Level and Intensity Calculations, (n.d.). ⟨http://www.lanl.gov/projects/feynman-center/deploying-innovation/intellectual-property/software-tools/relic/index.php⟩.
[4] A. Townshen, Principles of instrumental analysis, Anal. Chim. Acta 152 (1983) 314, https://doi.org/10.1016/S0003-2670(00)84936-3.
[5] J.D.L. Dutra, T.D. Bispo, R.O. Freire, LUMPAC lanthanide luminescence software: efficient and user friendly, J. Comput. Chem. 35 (2014) 772–775, https://doi.org/10.1002/jcc.23542.
[6] L. ačanin, S.R. Luki, D.M. Petrovi, M. Nikoli, M.D. Dramićanin, Judd–Ofelt analysis of luminescence emission from Zn_2SiO_4:Eu^{3+} nanoparticles obtained by a polymer-assisted sol–gel method, Phys. B Condens. Matter 406 (2011) 2319–2322, https://doi.org/10.1016/j.physb.2011.03.068.
[7] C. Görller-Walrand, K. Binnemans, Chapter 167 spectral intensities of f-f transitions, Handb. Phys. Chem. Rare Earths (1998) 101–264, https://doi.org/10.1016/S0168-1273(98)25006-9.
[8] W.T. Carnall, G.L. Goodman, K. Rajnak, R.S. Rana, A systematic analysis of the spectra of the lanthanides doped into single crystal LaF_3, J. Chem. Phys. 90 (1989) 3443–3457, https://doi.org/10.1063/1.455853.
[9] K. Binnemans, Interpretation of europium(III) spectra, Coord. Chem. Rev. 295 (2015) 1–45, https://doi.org/10.1016/j.ccr.2015.02.015.
[10] S.S. Babu, P. Babu, C.K. Jayasankar, W. Sievers, T. Tröster, G. Wortmann, Optical absorption and photoluminescence studies of Eu^{3+}-doped phosphate and fluorophosphate glasses, J. Lumin. 126 (2007) 109–120, https://doi.org/10.1016/j.jlumin.2006.05.010.
[11] M.G. Brik, Z.M. Antic, K. Vukovic, M.D. Dramicanin, Judd-Ofelt analysis of Eu^{3+} emission in TiO_2 anatase nanoparticles, Mater. Trans. 56 (2015) 1416–1418, https://doi.org/10.2320/matertrans.MA201566.
[12] D.F. Eaton, International union of pure and applied chemistry organic chemistry division commission on photochemistry, J. Photochem. Photobiol. B Biol. 2 (1988) 523–531, https://doi.org/10.1016/1011-1344(88)85081-4.
[13] M.H.V. Werts, R.T.F. Jukes, J.W. Verhoeven, The emission spectrum and the radiative lifetime of Eu^{3+} in luminescent lanthanide complexes, Phys. Chem. Chem. Phys. 4 (2002) 1542–1548, https://doi.org/10.1039/b107770h.
[14] M. Ferhi, C. Bouzidi, K. Horchani-Naifer, H. Elhouichet, M. Ferid, Judd–Ofelt analysis of spectroscopic properties of Eu^{3+} doped $KLa(PO_3)_4$, J. Lumin. 157 (2015) 21–27, https://doi.org/10.1016/j.jlumin.2014.08.017.
[15] J. Papan, D.J. Jovanović, K. Vuković, K. Smits, V. orđevi, M. Dramićanin, Europium (III)-doped $A_2Hf_2O_7$ (A = Y, Gd, Lu) nanoparticles: influence of annealing temperature, europium(III) concentration and host cation on the luminescent properties, Opt. Mater. 61 (2016) 68–76, https://doi.org/10.1016/j.optmat.2016.04.007.
[16] W.L. Barnes, R.I. Laming, E.J. Tarbox, P.R. Morkel, Absorption and emission cross section of Er/sup 3+/ doped silica fibers, IEEE J. Quantum Electron. 27 (1991) 1004–1010, https://doi.org/10.1109/3.83335.
[17] M.N. Polyanskiy, Refractive index database, (n.d.). ⟨https://refractiveindex.info⟩. (Accessed 5 March 2018).
[18] Origin, (n.d.). ⟨http://www.originlab.com⟩.
[19] S. Stojadinović, R. Vasilić, Formation and photoluminescence of Eu^{3+} doped zirconia coatings formed by plasma electrolytic oxidation, J. Lumin. 176 (2016) 25–31, https://doi.org/10.1016/j.jlumin.2016.03.012.
[20] S. Stojadinović, R. Vasilić, Orange–red photoluminescence of Nb_2O_5:Eu^{3+}, Sm^{3+} coatings formed by plasma electrolytic oxidation of niobium, J. Alloy. Compd. 685 (2016) 881–889, https://doi.org/10.1016/j.jallcom.2016.06.192.
[21] S. Stojadinovi, N. Radi, B. Grbi, S. Maleti, P. Stefanov, A. Pačevski, R. Vasilić, Structural, photoluminescent and photocatalytic properties of TiO_2:Eu^{3+} coatings formed by plasma electrolytic oxidation, Appl. Surf. Sci. 370 (2016) 218–228, https://doi.org/10.1016/j.apsusc.2016.02.131.
[22] M. Dejneka, E. Snitzer, R.E. Riman, Blue, green and red fluorescence and energy transfer of Eu^{3+} in fluoride glasses, J. Lumin. 65 (1995) 227–245, https://doi.org/10.1016/0022-2313(95)00073-9.
[23] N.B.D. Lima, J.D.L. Dutra, S.M.C. Gonçalves, R.O. Freire, A.M. Simas, Chemical partition of the radiative decay rate of luminescence of Europium complexes, Sci. Rep. 6 (2016) 21204, https://doi.org/10.1038/srep21204.
[24] K. Binnemans, C. Görller-Walrand, Application of Eu^{3+} ion for site symmetry determination, J. Rare Earths 14 (1996) 173–180.
[25] H.-Q. Liu, L.-L. Wang, S.-G. Chen, B.-S. Zou, Optical properties of nanocrystal and bulk ZrO_2:Eu^{3+}, J. Alloy. Compd. 448 (2008) 336–339, https://doi.org/10.1016/j.jallcom.2006.11.171.
[26] P.A. Tanner, Some misconceptions concerning the electronic spectra of tri-positive europium and cerium, Chem. Soc. Rev. 42 (2013) 5090, https://doi.org/10.1039/c3cs60033e.
[27] C. Wyman, P.-P. Sloan, P. Shirley, Simple analytic approximations to the CIE XYZ color matching functions, J. Comput. Graph. Tech. 2 (2013) 1–11 ⟨http://jcgt.org/published/0002/02/01/paper.pdf⟩.
[28] C. Abraham, A Beginner's Guide to (CIE) Colorimetry, 2016. ⟨https://medium.com/hipster-color-science/a-beginners-guide-to-colorimetry-401f1830b65a⟩. (Accessed April 3, 2018).
[29] Ligting Research Center, Appendix A: Calculating chromaticity coordinates, NLPIP - Specif. Reports, (n.d.). ⟨http://www.lrc.rpi.edu/programs/nlpip/lightinganswers/lightsources/appendixa.asp⟩. (Accessed 3 March 2018).
[30] A.N. Meza-Rocha, A. Speghini, M. Bettinelli, U. Caldiño, Orange and reddish-orange light emitting phosphors: Sm^{3+} and Sm^{3+}/Eu^{3+} doped zinc phosphate glasses, J. Lumin. 167 (2015) 305–309, https://doi.org/10.1016/j.jlumin.2015.06.050.
[31] Google Scholar, (n.d.). ⟨https://scholar.google.com⟩. (Accessed 1 January 2018).